

Diagrammatic description of a system coupled strongly to a bosonic bath

Michael Marthaler and Juha Leppäkangas

Institut für Theoretische Festkörperphysik, Karlsruhe Institute of Technology, D-76128 Karlsruhe, Germany

(Received 19 October 2015; published 7 October 2016)

We study a system-bath description in the strong-coupling regime where it is not possible to derive a master equation for the reduced density matrix by a direct expansion in the system-bath coupling. A particular example is a bath with significant spectral weight at low frequencies. Through a unitary transformation, it can be possible to find a more suitable small expansion parameter. Within such an approach, we construct a formally exact expansion of the master equation on the Keldysh contour. We consider a system diagonally coupled to a bosonic bath and expansion in terms of a nondiagonal hopping term. The lowest-order expansion is equivalent to the so-called $P(E)$ theory or noninteracting blip approximation. The analysis of the higher-order contributions shows that there are two different classes of higher-order diagrams. We study how the convergence of this expansion depends on the form of the spectral function with significant weight at zero frequency.

DOI: [10.1103/PhysRevB.94.144301](https://doi.org/10.1103/PhysRevB.94.144301)**I. INTRODUCTION**

System-bath approaches are commonly used in many fields of physics [1]. Particularly important is their use in quantum optics and quantum transport [2]. Generally, in a system-bath approach, one defines a “system” which contains a small number of degrees of freedom and a “bath” which contains a large number of degrees of freedom. The system and the bath are mostly coupled linearly, although different forms of coupling are also possible.

A common approach to solve this problem is to expand the time evolution of the full density matrix in the coupling between the system and the bath and trace out the bath degrees of freedom. This results in an effective equation of motion for the (reduced) density matrix of the system. The well-known examples are the Bloch-Redfield [3] and Lindblad [4] master equations. Both of these models require a weak coupling between the system and the bath. To be more precise, they require a bath correlator with a decay rate which is large compared to the effective system-bath coupling. However, if the system-bath coupling is strong, other approaches can be more useful. For two-level systems, a well-known approach is the polaron transformation [5–7], i.e., transformation into the bath-dressed system states. This was first introduced to study polaronic hopping of electrons with wave functions confined to single atomic sites [8]. Using the polaron transformation, the bath contribution is completely diagonalized. It is then necessary to expand in the terms of the original system Hamiltonian that do not commute with the system-bath coupling operator, dressed now by the bath operators. This approach is also known as the noninteracting blip approximation [9–11] (NIBA) and can be extended to the weakly interacting blip approximation [12,13].

It is not always straightforward to define the coupling strength between the system and the bath. In many cases, it is helpful to consider the spectral function of the bath modes to understand which method might work best. If the spectral function is very smooth, a direct expansion in the system-bath coupling is usually warranted. However, if the spectral function has sharp peaks, more care is necessary. A simple example is the spectral function $S(\omega) = \gamma\lambda^2/[\lambda^2 + (\omega - \omega_0)^2]$ (we use the notation $\hbar = 1$). If an energy splitting of the system is

close to the peak at $\omega = \omega_0$, it is possible to consider the height of the peak (γ) as the strength of the coupling, whereas the width of the peak (λ) gives us a good indication of the decay time of the bath correlator. Then, for $\gamma/\lambda \gg 1$, we are in the strong-coupling limit, and for $\gamma/\lambda \ll 1$, we are in the weak-coupling limit.

In this paper, we investigate a situation with a bath spectral density which has a substantial spectral weight at low frequencies. If the effect of temperature is considered, we will have a spectral function peaked at zero frequency which is exactly in the strong-coupling limit, i.e., its peak is higher than it is wide. As we will discuss later, this spectral function can be a result of coupling a quantum system to a large ohmic resistor [14], in which case we have an ohmic spectral density with small cutoff frequency. We will also discuss how our noise spectrum can be considered as a subcomponent of $1/f$ noise [15]. Furthermore, the spectral density relevant for our work has been measured, e.g., in flux qubits which are used in the D-Wave Systems devices [16,17]. In larger coupled systems containing these qubits, a description based on polaronic hopping has also already been studied [18].

This paper represents a continuation of our work on lasing in systems under strong noise [19,20] and incoherent Cooper-pair tunneling in Josephson-junction arrays [21]. In both cases, we used the lowest-order results of our expansion theory, and here we present the higher-order expansion which is used to analyze the convergence conditions. The same physics also governs inelastic Cooper-pair tunneling across voltage-biased Josephson junctions in the Coulomb blockade regime [14]. In this system, higher-order diagrams similar to what we consider in this paper have been formulated earlier by us and also explicitly evaluated beyond the leading order [22,23].

This paper is organized as follows. In Sec. II, we start by introducing our model in an abstract way and, in Sec. III, we discuss specific physical realizations where this expansion is applicable and has partially already been used. In Sec. IV, we introduce our expansion theory to all orders on the Keldysh contour. In Sec. V, we study the convergence conditions in the specific case of strong low-frequency noise, which can of course also be used to estimate the validity of the lowest-order expansion. We consider both the low- and high-temperature regimes. The conclusions and discussion are given in Sec. VI.

II. THE MODEL

We consider a system coupled diagonally to a bosonic bath in the presence of a nondiagonal hopping term, described by the total Hamiltonian

$$H_0 = H_D + (\hat{T} + \hat{T}^\dagger) + \hat{D} \sum_i c_i (\hat{b}_i^\dagger + \hat{b}_i) + \sum_i \omega_i \hat{b}_i^\dagger \hat{b}_i. \quad (1)$$

The system Hamiltonian consists of H_D , a Hamiltonian which commutes with the coupling operator \hat{D} , and a (hopping) part which does not commute with \hat{D} , given by $\hat{T} + \hat{T}^\dagger$. The system is coupled linearly to the bath of bosonic modes with frequencies ω_i , described by the corresponding annihilation (and creation) operators $\hat{b}_i^{(\dagger)}$. Here, the commutator between the operators \hat{T} and \hat{D} satisfies the property

$$[\hat{T}, \hat{D}] = c\hat{T}, \quad (2)$$

where c is a constant. In Sec. III, we introduce several systems whose Hamiltonians satisfy the above-mentioned properties.

Provided by Eq. (2), it is now convenient to do the unitary (polaron) transformation,

$$U_D = \exp \left[-\hat{D} \sum_i \frac{c_i}{\omega_i} (\hat{b}_i^\dagger - \hat{b}_i) \right], \quad (3)$$

and bring the resulting total Hamiltonian into the standard form of a system-bath approach,

$$H = U_D^\dagger H_0 U_D = H_S + H_C + H_B, \quad (4)$$

with

$$H_S = H_D - \hat{D}^2 \sum_i \frac{c_i^2}{\omega_i}, \quad (5)$$

$$H_C = \hat{T} e^{-\hat{\phi}} + \hat{T}^\dagger e^{\hat{\phi}}, \quad \hat{\phi} = c \sum_i \frac{c_i}{\omega_i} (\hat{b}_i^\dagger - \hat{b}_i), \quad (6)$$

$$H_B = \sum_i \omega_i \hat{b}_i^\dagger \hat{b}_i. \quad (7)$$

The system Hamiltonian H_S consists of H_D (introduced above) and a renormalization coming from the bath. Coupling to the bath is described by H_C and the bath Hamiltonian H_B remains unchanged. It will now be our goal to derive a master equation by expanding the equation of motion for the reduced density matrix in orders of H_C . For example, when applied to the spin-boson model or to a Josephson junction coupled to an electromagnetic environment, this corresponds to an expansion of the system dynamics in powers of the tunneling coupling, as discussed below.

III. PHYSICAL REALIZATIONS

In this section, we introduce specific physical realizations where our expansion is applicable. The specific form of diagrammatic expansion, the leading-order master equation, and its convergence analysis are then given in Secs. IV and V.

Generally, prior to the unitary transformation, the system Hamiltonian and the coupling Hamiltonian can be described

by diagonal contributions,

$$H_D = \sum_n \epsilon_n |n\rangle \langle n|, \quad (8)$$

and similarly for the coupling to the bath,

$$\hat{D} = \sum_n d_n |n\rangle \langle n|. \quad (9)$$

In the following, we will consider an off-diagonal part with (hopping) coupling between the nearest system levels,

$$\hat{T} = \sum_n \tau_n |n\rangle \langle n+1|. \quad (10)$$

For our theory to be applicable, that is, for Eq. (2) to be valid, the matrix elements d_n need to have the property $d_{n+1} - d_n = c$. We point out that the approach can also be extended to more complicated operators \hat{T} . Let us now discuss some important models from the literature which can be mapped to the Hamiltonian of Eq. (1).

A. Spin-boson model

One of the most well-studied problems in system-bath physics is the spin-boson model [24,25]. It describes many interesting systems and phenomena, such as electron-transfer reactions [26], biomolecules [27], cavity QED [28,29], and general dissipative quantum systems [30,31]. The Hamiltonian is given by

$$H = \frac{1}{2} \epsilon \hat{\sigma}_z - \frac{1}{2} \Delta \hat{\sigma}_x + \hat{\sigma}_z \sum_i c_i (\hat{b}_i^\dagger + \hat{b}_i) + \sum_i \omega_i \hat{b}_i^\dagger \hat{b}_i. \quad (11)$$

Here, $\hat{\sigma}_i$ are the Pauli matrices acting on a two-level system. This can be mapped onto the Hamiltonian of Eq. (1), with identification

$$H_D = \frac{1}{2} \epsilon \hat{\sigma}_z, \quad \hat{T} = -\frac{1}{2} \Delta \hat{\sigma}_+, \quad D = \hat{\sigma}_z. \quad (12)$$

We introduced the spin raising and lowering operators $\hat{\sigma}_+ + \hat{\sigma}_- = \hat{\sigma}_x$. For the spin-boson model, an expansion in terms of \hat{T} in lowest order is known as the noninteracting blip approximation [9]. Higher-order expansions have also been formulated [12,13].

B. Jaynes-Cummings model

The Jaynes-Cummings model describes an interaction between a single electromagnetic mode and a two-level system. If the two-level system is coupled to a bosonic bath (e.g., to describe decoherence), the total Hamiltonian is given by

$$H = \frac{1}{2} \epsilon \hat{\sigma}_z + g (\hat{\sigma}_+ \hat{a} + \hat{\sigma}_- \hat{a}^\dagger) + \omega \hat{a}^\dagger \hat{a} + \hat{\sigma}_z \sum_i c_i (\hat{b}_i^\dagger + \hat{b}_i) + \sum_i \omega_i \hat{b}_i^\dagger \hat{b}_i. \quad (13)$$

This model has been studied by us in the context of inversionless lasing [19] and coupling of quantum dots to a transmission-line resonator [20,32]. We have here

$$H_D = \frac{1}{2} \epsilon \hat{\sigma}_z + \omega \hat{a}^\dagger \hat{a}, \quad \hat{T} = g \hat{a} \hat{\sigma}_+, \quad \hat{D} = \hat{\sigma}_z. \quad (14)$$

When expanding in \hat{T} , one has to note that the expansion parameter grows with the photon number. Therefore, it is clear that a lowest-order approximation is only valid for small photon numbers (small $g\sqrt{n}$ compared to ω , where n is the resonator photon number).

C. Superconducting devices in the charge regime

Another system of great interest where the above discussion is valid is superconducting devices in the charge regime. As an example, the Hamiltonian of a superconducting charge qubit connected (capacitively) to a transmission line can be written in the form

$$H = E_C \hat{N}^2 - E_J \cos \hat{\theta} + \hat{N} \sum_i c_i (\hat{b}_i^\dagger + \hat{b}_i) + \sum_i \omega_i \hat{b}_i^\dagger \hat{b}_i. \quad (15)$$

Here, \hat{N} is the excess Cooper-pair number on the island with Cooper-pair charging energy E_C , and E_J is the Josephson coupling describing Cooper-pair tunneling between the island and the lead. The superconducting phase and the charge operator are conjugate variables and satisfy $[\hat{N}, e^{i\hat{\theta}}] = e^{i\hat{\theta}}$, which means that we can identify

$$H_D = E_C \hat{N}^2, \quad \hat{T} = -E_J e^{i\hat{\theta}}/2, \quad \hat{D} = \hat{N}. \quad (16)$$

For this case, the lowest-order expansion is equivalent to the $P(E)$ theory [14]. In this system, expansion schemes to higher-orders in E_J have also been considered by us and others [22,23,33,34]. Naturally, many other noise sources, such as subgap quasiparticles [35,36], can have an effect on superconducting systems. In the limit of large E_J , the noise characteristics of this model can also change substantially [37] and, for highly structured environments, open system methods have been discussed [38].

D. Multipartite systems

The model presented here can also easily be extended to include coupling of many system operators to independent baths. Here each of the system operators has to have a similar relation with the system Hamiltonian as in Eq. (2). In particular, this model can be used to study incoherent Cooper-pair tunneling in Josephson-junction arrays [21,39] and it could also be useful when considering hopping between many coupled two-level systems with low coherence [40,41].

IV. EXPANSION ON THE KELDYSH CONTOUR

The total Hamiltonian H is divided into three parts: the quantum system H_S , the bath H_B , and the coupling between the quantum system and the bath H_C ; see Eqs. (4)–(7). Our aim now is to derive an equation of motion for the reduced density matrix for the quantum system, where we trace out the degrees of freedom of the bath. The expansion of the time evolution on Keldysh contour is discussed extensively in the literature; see, for example, Ref. [42]. Below, we will give a short review of the relevant steps. Differences to usual approaches appear when we introduce the contraction method of exponentialized bosonic operators (Sec. IV B).

A. Time evolution of the reduced density matrix

We start with the equation of motion for the average value of the projection operator $\hat{P}_{ss'}$, where $|s\rangle$ are the eigenstates of H_S . We have then

$$\hat{P}_{ss'} = |s'\rangle\langle s|, \quad H_S |s\rangle = E_s |s\rangle. \quad (17)$$

In this notation, we can define the elements of the reduced density matrix as

$$P_{ss'}(t) = \langle \hat{P}_{ss'}(t) \rangle. \quad (18)$$

The time evolution is then given by

$$P_{ss'}(t) = \text{Tr}[\hat{\rho}(t_0) \hat{U}_1^\dagger(t, t_0) \hat{P}_{ss',1}(t) \hat{U}_1(t, t_0)]. \quad (19)$$

This approach is equivalent to the Nakajima-Zwanziger projection formula [1]. Here we use the definition of an operator \hat{O} in the interaction picture,

$$\hat{O}_I(t) = e^{i(H_S+H_B)(t-t_0)} \hat{O} e^{-i(H_S+H_B)(t-t_0)}. \quad (20)$$

The time-evolution operator in the interaction picture is given by

$$U_I(t, t_0) = \mathcal{T} e^{-i \int_{t_0}^t H_{C,1}(t') dt'}, \quad (21)$$

where \mathcal{T} is the time-ordering operator ($t > t_0$).

We assume now that at time t_0 , the density matrix separates into the density matrix of the bath $\hat{\rho}_B(t_0)$ and system $\hat{\rho}_S(t_0)$, and we write it in the form

$$\hat{\rho}(t_0) = \hat{\rho}_B(t_0) \hat{\rho}_S(t_0) = \hat{\rho}_B \sum_{\bar{s}\bar{s}'} P_{\bar{s}\bar{s}'}(t_0) |\bar{s}\rangle\langle\bar{s}'|. \quad (22)$$

Combining Eqs. (19) and (22) allows us to write

$$P_{ss'}(t) = \sum_{\bar{s}\bar{s}'} P_{\bar{s}\bar{s}'}(t_0) \Pi_{\bar{s}\bar{s}' \rightarrow ss'}(t_0, t), \quad (23)$$

with the time evolution of the superoperator $\Pi(t_0, t)$. Expanding the time-evolution operators as in Eq. (21) gives us

$$\begin{aligned} & \Pi_{\bar{s}\bar{s}' \rightarrow ss'}(t_0, t) \\ &= \langle \bar{s}' | \text{Tr}_B \rho_B(t_0) \sum_{m=0}^{\infty} (-i)^m \int_{t_0}^t dt'_1 \int_{t_0}^{t'_1} dt'_2 \cdots \\ & \quad \cdots \int_{t_0}^{t'_{m-1}} dt'_m \mathcal{T}_K [H_{C,1}(t'_1) H_{C,1}(t'_2) \cdots H_{C,1}(t'_m) \hat{P}_{ss',1}(t)] | \bar{s} \rangle. \end{aligned} \quad (24)$$

Here, \mathcal{T}_K represents the time sorting *along the Keldysh contour*, which we will explain below.

The Keldysh contour has two branches. The upper branch represents the time evolution from t_0 to t , and the lower branch represents time evolution in the opposite direction. In our case, the time t is determined by the projection operator $\hat{P}_{ss',1}(t)$. All operators to the right of $\hat{P}_{ss',1}(t)$ will be on the upper branch of the Keldysh contour, and all operators to the left will be on the lower branch. Each lower-branch operator will be associated with an extra factor -1 .

In the coupling Hamiltonian H_C , we have the operators $\hat{T} e^{-\hat{\phi}(t)}$ and $\hat{T}^\dagger e^{\hat{\phi}(t)}$; see Eq. (6). We separate these two terms in our description of the expansion on the Keldysh contour. The operators $\hat{T} e^{-\hat{\phi}(t)}$ are represented by filled circles, while

$\hat{T}^\dagger e^{\hat{\phi}(t)}$ are represented by empty circles. On the Keldysh contour, the time evolution of the superoperator is then given by the following:

$$\Pi(t_0, t) = \sum_{m=0}^{\infty} i^m \text{Diagram} \quad (25)$$

Here, for each order m , a summation over all geometrically different diagrams is made.

To define a self-energy, we will now establish contraction rules for correlators of the form

$$\begin{aligned} \text{Tr}_B[\hat{\rho}_B(t_0) \mathcal{T}_K e^{\hat{\phi}_1} e^{-\hat{\phi}_2} e^{\hat{\phi}_3} \dots e^{\hat{\phi}_m}] \\ = \langle \mathcal{T}_K e^{\hat{\phi}_1} e^{-\hat{\phi}_2} e^{\hat{\phi}_3} \dots e^{\hat{\phi}_m} \rangle_B \\ = \langle e^{\hat{\phi}_m} e^{-\hat{\phi}_{m-2}} \dots e^{-\hat{\phi}_2} e^{\hat{\phi}_1} e^{\hat{\phi}_3} \dots e^{-\hat{\phi}_{m-1}} \rangle_B, \end{aligned} \quad (26)$$

where the time ordering of the lowest line corresponds to the diagram in Eq. (25). We have used the notation $\hat{\phi}(t_i) \equiv \hat{\phi}_i$. It is the next step, which is different from usual master equation derivations. This is because the Wick's theorem does not apply to operators of the type $\exp[\hat{\phi}_i]$ and we cannot rewrite this m -time correlator in products of two-time correlators in the usual way.

B. Contraction rules

The Feynman disentangling method allows us to derive a helpful simplification for ensemble averages of products of operators $\exp(\hat{\phi}_n)$, where $\hat{\phi}_n$ is an arbitrary linear combination of bosonic annihilation and creation operators. The disentangling has the form

$$\langle e^{n_1 \hat{\phi}_1} e^{n_2 \hat{\phi}_2} \dots e^{n_m \hat{\phi}_m} \rangle = e^{\frac{1}{2} (\sum_{i=1}^m n_i \hat{\phi}_i)^2} e^{\frac{1}{2} \sum_{i < j} [n_i \hat{\phi}_i, n_j \hat{\phi}_j]}. \quad (27)$$

Here, the factors n_i take values ± 1 . This result can also be derived by applying the Wick's theorem to Taylor expansions of the exponentialized operators, similarly as in Ref. [14]. Using Eq. (27), it is straightforward to show that averaging products over the reservoir is only nonzero if there is the same number of operators with opposite signs of the exponents. Therefore, we only have to consider diagrams with an equal amount of filled and empty circles. For such combinations, we can write

$$\begin{aligned} \langle \mathcal{T}_K \Pi_n e^{\hat{\phi}_n} e^{-\hat{\phi}_{n'}} \rangle = e^{\frac{1}{2} (\sum_n (\hat{\phi}_n - \hat{\phi}_{n'})^2)} e^{-\frac{1}{2} \sum_{n < n'} \mathcal{T}_K [\hat{\phi}_n, \hat{\phi}_{n'}]} \\ \times e^{\frac{1}{2} \sum_{n < m} \mathcal{T}_K [\hat{\phi}_n, \hat{\phi}_m]} e^{\frac{1}{2} \sum_{n' < m'} \mathcal{T}_K [\hat{\phi}_{n'}, \hat{\phi}_{m'}]}. \end{aligned} \quad (28)$$

Here we use the notation where the number i (i') corresponds to a positive (negative) signed phase operator.

In the next step, we group all $e^{\hat{\phi}_n}$ to the $e^{-\hat{\phi}_{n'}}$ closest to each other on the real-time axis. The difference from the usual diagrammatic formulations is that each circle is paired only once. This is done practically by grouping the time-wise earliest empty circle to the time-wise earliest filled circle, and so on. This is the only possible way to connect the diagrams that allows for a consistent definition of a self-energy. For example, the lowest-order contribution to the self-energy will

contain exactly two vertices: one empty and one filled. This contribution has to be repeated n times for a diagrammatic part which contains n self-energies. Therefore, we have to connect the corresponding circles in diagrams with $2n$ vertices to reproduce the n lowest-order contractions. We will discuss this further below for a specific example.

Interactions beyond the pairings are included by pair connectors, introduced below. To write the resulting correlators in a compact form, we introduce the notation

$$f(\mathcal{T}_K [t_1, t_2, t_3, \dots]) = f(t_1, t_2, t_3, \dots). \quad (29)$$

The expression $\mathcal{T}_K [t_1, t_2, t_3, \dots]$ implies that the arguments of the function f should be time sorted along the Keldysh contour. For the particular example in Eq. (29), we assumed $t_1 > t_2 > t_3, \dots$ along the Keldysh contour.

We then separate contributions from the time-wise nearby pairs (introduced above) from other terms, which will describe interaction between these pairs. This allows us to bring the correlator into the form

$$\begin{aligned} \langle \mathcal{T}_K \Pi_n e^{\hat{\phi}_n} e^{-\hat{\phi}_{n'}} \rangle \\ = \Pi_n \langle \mathcal{T}_K e^{\hat{\phi}_n} e^{-\hat{\phi}_{n'}} \rangle \Pi_{n < m} \{ F(\mathcal{T}_K [t_n, t_{n'}, t_m, t_{m'}]) + 1 \} \\ = \Pi_n P(\mathcal{T}_K [t_n, t_{n'}]) \\ + \Pi_n P(\mathcal{T}_K [t_n, t_{n'}]) F(\mathcal{T}_K [t_2, t_2', t_1, t_1']) + \dots \end{aligned} \quad (30)$$

The two-time correlator $P(t_1, t_2)$ has the form

$$P(t_1, t_2) = \langle e^{\hat{\phi}(t_1)} e^{-\hat{\phi}(t_2)} \rangle = e^{C(t_1 - t_2)}. \quad (31)$$

Here, the pair correlator $C(t)$ is related to the bath structure as

$$\begin{aligned} C(t) = \frac{c^2}{\pi} \int_0^\infty d\omega \frac{J(\omega)}{\omega^2} \\ \times \left[\coth \left(\frac{\omega}{2k_B T} \right) (\cos \omega t - 1) - i \sin \omega t \right], \end{aligned} \quad (32)$$

where we have taken the continuum limit by defining $\pi \sum_i c_i^2 f(\omega_i)/\omega_i^2 \equiv \int d\omega J(\omega) f(\omega)/\omega^2$, for an arbitrary function $f(\omega)$. The Fourier transform of Eq. (31) is known from the $P(E)$ theory [14],

$$P(E) = \frac{1}{2\pi} \int_{-\infty}^\infty dt e^{C(t) + iEt}. \quad (33)$$

It satisfies $\int_{-\infty}^\infty P(E) dE = 1$ and describes the probability to exchange energy E with the bosonic environment in an incoherent transition between two system states connected by \hat{T} or \hat{T}^\dagger . As discussed in more detailed in Sec. V, the function $J(\omega)$ is related to the real part of the environmental impedance $Z(\omega)$ as $J(\omega) = 2\pi \omega \text{Re}[Z(\omega)]/R_Q$, where $R_Q = h/e^2$ is the resistance quantum.

The interaction between the pairs is described by the function

$$F(\mathcal{T}_K [t_n, t_{n'}, t_m, t_{m'}]) = e^{\langle \mathcal{T}_K (\hat{\phi}_n - \hat{\phi}_{n'}) (\hat{\phi}_m - \hat{\phi}_{m'}) \rangle} - 1, \quad (34)$$

where the first term on the right-hand side collects all the terms describing interaction between two pairs. Notice the addition and subtraction of 1 when inserted into the full correlator in Eq. (30): the contribution beyond 1 (function

F) describes deviations from Gaussian contractions. This definition is sound, since at finite temperatures and in the long-time limit, the function F decays exponentially to zero with increasing time separation between the two pairs. We call the function $F(\mathcal{T}_K[t_n, t_{n'}, t_m, t_{m'}])$ the *connector*.

We are now ready to go forward in using our diagrammatic formulation of the problem. As an example, we show a contraction of an element of the time evolution, with four vertices:

$$\text{Diagram with 4 vertices} = \text{Diagram 1} + \text{Diagram 2} \quad (35)$$

Here the dashed line describes a connector between the pair correlators (wiggled lines). We see how a diagram with four vertices is contracted in a way which reproduces the lowest-order diagrams twice, which is necessary to allow for a consistent definition of the self-energy. Our contraction rule is the only possible rule which allows for such a consistent definition.

As another example, we show a contraction of an element of the time evolution with six vertices:

$$\text{Diagram with 6 vertices} = \text{Diagram 1} + \text{Diagram 2} + \text{Diagram 3} + \dots \quad (36)$$

Again, the first contraction on the right-hand side reproduces the lowest-order diagram three times and the second contraction reproduces a combination of the first two diagrams in the previous diagram, and so on.

C. Self-energy

Since all of the diagrams are separable or inseparable [42], we can now define the self-energy consisting of all inseparable diagrams (diagrams that cannot be cut into two by a vertical line without crossing a wiggled or a dashed line). In the diagrammatic form, it can be written as

$$\Sigma = \text{Diagram 1} + \dots + \text{Diagram 2} + \dots + \text{Diagram 3} + \dots \quad (37)$$

Using the self-energy, we can write the time evolution $\Pi(t_0, t)$ as follows:

$$\begin{aligned} \Pi(t_0, t) &= \text{Diagram 1} + \boxed{\Sigma} + \boxed{\Sigma} \boxed{\Sigma} \\ &+ \boxed{\Sigma} \boxed{\Sigma} \boxed{\Sigma} + \dots \\ &= \text{Diagram 1} + \boxed{\Sigma} \Pi \end{aligned} \quad (38)$$

Using the above Dyson equation, we get the equation of motion for the reduced density matrix,

$$\partial_t \hat{P}(t) = i[\hat{P}(t), H_S] + \int_{t_0}^t \Sigma(t', t) \hat{P}(t') dt', \quad (39)$$

which is, in principle, exact. Obviously, the key difficulty here is the calculation of the self-energy, $\Sigma(t', t)$.

D. Leading-order master equation

We will now derive the leading-order approximation for the equation of motion of the density matrix. The self-energy in the leading order is a sum of all eight second-order diagrams, which have the following form:

$$\Sigma = \text{Diagram 1} + \text{Diagram 2} + \text{Diagram 3} + \text{Diagram 4} + \text{Diagram 5} + \text{Diagram 6} + \text{Diagram 7} + \text{Diagram 8} \quad (40)$$

By evaluating each contribution explicitly, we can write down the master equation. As an example, we evaluate the contribution from the first diagram,

$$\Sigma_{\bar{s}\bar{s}' \rightarrow s s'}(t', t) = \langle \bar{s}' | \hat{T} | s' \rangle \langle s | \hat{T}^\dagger | \bar{s} \rangle P(t', t) e^{i(E_{s'} - E_{\bar{s}})(t - t')}.$$

In the Markov approximation, one neglects memory effects in the system time evolution, which means that in Eq. (39) the density matrix $\hat{P}(t')$ is replaced by the free evolution $e^{iH_S(t-t')} \hat{P}(t) e^{-iH_S(t-t')}$. This is a convenient but not necessary approximation to be done here. The Markov approximation is equivalent to the analysis of the crossing diagrams [43]. If the function $P(t_1, t_2)$ decays fast, such as in the high-temperature limit considered in Sec. V A, the Markov approximation is well justified. This allows for a straightforward integration of the equations over the time t' , giving generalized transition rates of the form

$$\begin{aligned} \Gamma(E) &\equiv \int_{-\infty}^t dt' P(t', t) e^{-iE(t-t')} \\ &= \int_{-\infty}^t dt' e^{C(t'-t)} e^{iE(t-t')} = \pi P(E) + iR(E). \end{aligned} \quad (41)$$

Here, the first term on the right-hand side is purely real and corresponds to the $P(E)$ function defined in Eq. (33). This describes incoherent transitions with energy exchange with the environment. The second term is purely imaginary and corresponds to energy renormalization effects. These are usually neglected or included in the system Hamiltonian. They can result in important observable effects [44]. This term can be written in the form

$$R(E) = -\mathcal{P} \int_{-\infty}^{\infty} d\omega \frac{P(E + \omega)}{\omega}, \quad (42)$$

where \mathcal{P} indicates that the integration is made as a principal value around $\omega = 0$.

In total, after summing over all eight diagrams, one obtains the well-known Bloch-Redfield equations of motion [1,3],

$$\dot{P}_{s s'}(t) = -i(E_s - E_{s'}) P_{s s'}(t) + \sum_{\bar{s} \bar{s}'} \Pi_{\bar{s} \bar{s}' s s'}(t), \quad (43)$$

where the performed unitary transformation affects the form of the generalized transition rates,

$$\begin{aligned} \Pi_{\bar{s}\bar{s}'s s'}(t) &= \Gamma_{\bar{s}'s'}[T_{\bar{s}\bar{s}}^\dagger T_{\bar{s}'s'} + T_{s\bar{s}} T_{\bar{s}'s'}^\dagger]P_{\bar{s}\bar{s}'}(t) \\ &+ \Gamma_{\bar{s}s}^*[T_{\bar{s}\bar{s}}^\dagger T_{\bar{s}'s'} + T_{\bar{s}\bar{s}} T_{\bar{s}'s'}^\dagger]P_{\bar{s}\bar{s}'}(t) \\ &- \sum_v \Gamma_{\bar{s}v}^*[T_{\bar{s}v}^\dagger T_{v\bar{s}'} + T_{sv} T_{v\bar{s}}^\dagger]P_{\bar{s}\bar{s}'}(t)\delta_{\bar{s}'s'} \\ &- \sum_v \Gamma_{\bar{s}'v}[T_{\bar{s}'v}^\dagger T_{v\bar{s}} + T_{\bar{s}'v} T_{v\bar{s}'}^\dagger]P_{\bar{s}\bar{s}'}(t)\delta_{\bar{s}s}, \end{aligned}$$

with $T_{ij} \equiv \langle i|\hat{T}|j\rangle$ and $\Gamma_{ij} \equiv \Gamma(E_i) - \Gamma(E_j)$.

The leading-order master equation under the polaron transformation is a useful and straightforward tool for many systems. Our previous studies include lasing under strong noise [19,20] and incoherent Cooper-pair tunneling in Josephson-junction arrays [21]. The diagrammatic formulation of higher orders derived in the preceding sections then allows us to study convergence criteria, performed in Sec. V.

V. STRONG LOW-FREQUENCY NOISE AND CONDITIONS FOR CONVERGENCE

In the preceding section, we presented a diagrammatic expansion of the time evolution of the density matrix and derived the master equation in the leading order. Here, we want to discuss the conditions for the leading-order expansion to be valid. For this, we first want to introduce a specific model for the spectral function.

We consider a case which is often discussed within $P(E)$ theory [14], where the spectral function can be related to an impedance $Z(\omega)$ via

$$J(\omega) = 2\pi\omega \frac{\text{Re}[Z(\omega)]}{R_Q}, \quad (44)$$

where $R_Q = h/e^2$ is the resistance quantum. If our system has a dipole moment and is capacitively coupled to an ohmic environment, the impedance can take the form

$$\text{Re}[Z(\omega)] = \frac{R}{1 + (\omega RC)^2}. \quad (45)$$

Here, R characterizes the dissipation of the environment and the capacitance C defines a cutoff frequency $\omega_R = 1/RC$. The spectral density in this case can also be written as

$$J(\omega) = 2\epsilon_C\omega \frac{\omega_R}{\omega^2 + \omega_R^2}, \quad (46)$$

with the charging energy $\epsilon_C = e^2/2C$.

A. Cutoff frequencies smaller than temperature

If we consider the occupation of the modes by finite temperature $k_B T$, for small cutoff frequencies, $\omega_R \ll k_B T$, we get a spectral function,

$$S(\omega) = J(\omega) \coth(\omega/2k_B T) \approx \frac{4\epsilon_C k_B T \omega_R}{\omega^2 + \omega_R^2}. \quad (47)$$

This spectral function has a maximum at $\omega = 0$ and therefore the noise we are considering is low-frequency noise. The spectral function is characterized by height $\epsilon_C k_B T / \omega_R$ and

width ω_R . This can be an important regime, even at milli-Kelvin temperatures [16,21,22], since cutoff frequencies can be even smaller.

1. Contraction function

We now further study the spectral density of Eq. (46) in the limit $\omega_R \ll k_B T$. The corresponding contraction function $P(t_1, t_2)$ [see Eqs. (31) and (32)] has the form

$$P(t_1, t_2) = \exp \left\{ -\frac{2c^2 \epsilon_C k_B T (1 - e^{-\omega_R |\delta t|} - \omega_R |\delta t|)}{\omega_R^2} - i \frac{2c^2 \epsilon_C (1 - e^{-\omega_R |\delta t|})}{\omega_R} \text{Sign}(\delta t) \right\}. \quad (48)$$

Here we have defined $\delta t = t_1 - t_2$. The real part behaves quadratically at short times and linearly at long times. A characteristic time for the cross over is $1/\omega_R = RC$. The result for the imaginary part does not depend on temperature and is general.

We will now use the coupling $c = 1$; for other values, all the results can be obtained by the change $\epsilon_C \rightarrow c^2 \epsilon_C$. In the strong-coupling limit, $\omega_R \ll \sqrt{\epsilon_C k_B T}$, we can use the short-time approximation and the relevant behavior simplifies to [45]

$$P(t_1, t_2) \approx \exp\{-\epsilon_C [k_B T (t_1 - t_2)^2 + i(t_1 - t_2)]\}. \quad (49)$$

This also implies that we consider a spectral function which is sharply peaked at small frequencies.

We note that when using only quadratic approximation for correlation functions, the corresponding coupling between the pairs (F function) does not go to zero with increasing the distance between pairs. However, it does go to zero when the linear behavior of Eq. (48) dominates ($t > RC$). This is also seen in the convergence results derived below.

It should also be noted that there is a direct relation between the spectral function (47) and $1/f$ noise [15]. It is known that $1/f$ noise can be described by many superimposed Lorentzian spectra, with a probability distribution for the width ω_R which is given by $1/\omega_R$,

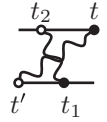
$$S_{1/f}(\omega) = \int_0^\infty d\omega_R \frac{1}{\omega_R} S(\omega) = \frac{2\pi \epsilon_C k_B T}{\omega}. \quad (50)$$

As we will see later, the expansion we discuss here can accommodate low-frequency noise of the type described by Eq. (47) for rather small cutoff frequencies ω_R , but not for $\omega_R \rightarrow 0$.

2. Analysis of higher-order diagrams

We assume strong coupling to the environment and therefore we assume large $\sqrt{k_B T \epsilon_C}$ compared to ω_R . In this case, $P(t_1, t_2)$ decays quickly and allows for the Markov approximation in the leading-order master equation. However, in contrast to the expansion studied in, e.g., Ref. [43], we have different classes of higher-order diagrams which decay in different ways.

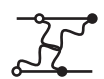
We analyze higher-order diagrams to understand the convergence conditions of our expansion. At first we will consider a standard diagram with two crossed contractions,



$$= m^4 \int_{t'}^t dt_1 \int_{t'}^{t_1} dt_2 P(t, t_2) P(t', t_1) \quad (51)$$

Here, the term $P(t, t_2)$ corresponds to the upper pair and $P(t', t_1)$ corresponds to the lower one. We assume that the relevant system energy splittings are small. If a system energy splitting is large, we get additional oscillating functions which improve convergence; therefore we are considering the worst-case scenario. The prefactor is given by the assumption that there is a characteristic energy scale m which corresponds to the relevant matrix element $m \propto \langle n | \hat{T} | n' \rangle$, where $|n\rangle$ and $|n'\rangle$ are eigenstates of the system.

In a rough approximation, where we also neglect the oscillating part in the contraction of Eq. (49) and assume that $t - t'$ is relatively large, we find



$$\approx -\sqrt{\frac{\pi}{2}} \frac{m^4 e^{-\frac{1}{2}\epsilon_C k_B T (t-t')^2}}{(\epsilon_C k_B T)^{3/2} (t-t')} \quad (52)$$

If we now compare the size of the lowest-order diagram with these results, we see that we need

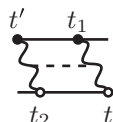
$$\frac{m^2}{\sqrt{\epsilon_C k_B T}} \gg \frac{m^4}{(\epsilon_C k_B T)^{3/2}}. \quad (53)$$

This gives us the rule for convergence,

$$\frac{m}{\sqrt{\epsilon_C k_B T}} \ll 1. \quad (54)$$

Basically, we see that the higher-order diagram of the form (52) can be neglected if the contraction $P(t_1, t_2)$ has a decay rate which is much larger than the coupling constant m . This is a well-known rule which applies for many expansion theories.

In the limit we are considering, at first sight it seems as if the cutoff frequency of the spectral function plays no role in the convergence. However, this is essential for different sets of diagrams, which have no crossing contractions but are inseparable because of a connector. These terms have the form



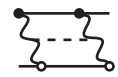
$$= m^4 \int_{t'}^t dt_1 \int_{t'}^{t_1} dt_2 P(t, t_1) P(t_2, t') F(t_2, t, t_1, t') \quad (55)$$

Diagrams of this form have also been shown to be relevant for the calculation of the statistics of photon emission in voltage-biased Josephson junctions [22,23]. Here, the function $P(t, t_1)$ describes the time-wise later pair and the function $P(t_2, t')$ describes the earlier one, whereas $F(t_2, t, t_1, t')$ describes the interaction between the two. We know that the functions $P(t_1, t)$ and $P(t', t_2)$ decay very fast. Therefore, we expand the connector F around $t_1 = t$ and $t_2 = t'$ using the Taylor expansion. This is again a valid approximation for relatively large $t - t'$. The lowest-order nonzero element of

this expansion is given by

$$\left. \frac{\partial F}{\partial t_1 \partial t_2} \right|_{t_1=t, t_2=t'} = -\frac{1}{\pi} \int_0^\infty d\omega J(\omega) \coth\left(\frac{\omega}{2k_B T}\right) \times [\cos \omega(t-t') - i \sin \omega(t-t')]. \quad (56)$$

In this approximation, we can write the diagram (55) in the form



$$= -m^4 \left. \frac{\partial^2 F}{\partial t_1 \partial t_2} \right|_{t_1=t, t_2=t'} \times \int_{t'}^t dt_1 \int_{t'}^{t_1} dt_2 P(t, t_1) (t-t_1) P(t_2, t') (t_2-t'). \quad (57)$$

Integration over the times gives us

$$\lim_{t-t' \rightarrow \infty} \int_{t'}^t dt_1 \int_{t'}^{t_1} dt_2 P(t_1, t) (t_1-t) P(t', t_2) (t_2-t') = \frac{1}{\epsilon_C^2 (k_B T)^2}. \quad (58)$$

Using the approximation for our spectral density in Eq. (46) as specified in Eq. (47), we can analytically estimate the contribution from the connector,

$$\left. \frac{\partial^2 F}{\partial t_1 \partial t_2} \right|_{t_1=t, t_2=t'} = 2\epsilon_C k_B T e^{-\omega_R(t-t')}. \quad (59)$$

This analysis implies that for relatively large times $t - t'$, the connector decays as the memory (RC) time of the environment. From this, we find the order of magnitude of the contribution of the diagram (55), which becomes $m^4 / \epsilon_C k_B T \omega_R$. If we compare this to the contribution of the lowest-order diagram, we find the convergence rule

$$\frac{m^2}{\omega_R \sqrt{\epsilon_C k_B T}} \ll 1. \quad (60)$$

From Eq. (60), we see that a noise source with a rather small cutoff frequency can in fact be treated, as long as the overall noise magnitude is sufficiently large. We also see that in the limit $\omega_R \rightarrow 0$, the expansion does not converge. This is natural since in this limit the memory time of the environment approaches infinity. In summary, we see that the bath cutoff frequency also plays an essential role in convergence of the expansion.

B. Convergence for temperatures smaller than cutoff frequency

With a similar analysis, we can also study the convergence in the case of strong coupling of the environment and small cutoff frequencies, but temperatures even smaller than the cutoff frequency, $\omega_R > k_B T$. The width of the spectral function is characterized now by $k_B T$, meaning that the strong-coupling limit corresponds to $\epsilon_C \gg \omega_R$, which is equivalent to $R \gg R_Q$. In this case, the result for the contraction function $P(t_1, t_2)$ can be derived from the formally exact solution given in Ref. [33]. We find a solution for the real part in the short- and long-time

limits,

$$\operatorname{Re}[P(t_1, t_2)] = \begin{cases} \exp\left\{-\frac{\epsilon_C}{\pi\omega_R}[\gamma - \cosh(\omega_R t)\operatorname{chi}(\omega_R t) + \sinh(\omega_R t)\operatorname{shi}(\omega_R t)]\right\}, & k_B T t \ll 1 \\ \exp\left[\frac{\epsilon_C k_B T}{\omega_R} t - \frac{\epsilon_C(H - \frac{\omega_R}{2k_B T\pi} + H \frac{\omega_R}{2k_B T\pi} - \pi \cot(\omega_R/2k_B T))}{2\pi\omega_R}\right], & k_B T t \gg 1, \end{cases} \quad (61)$$

where H_n is the harmonic number and $\operatorname{chi}(x)$ and $\operatorname{shi}(x)$ are the \cosh and \sinh integrals, respectively. For $T = 0$, the short-time limit is, in fact, the correct result at all times. In this case, our expansion will diverge and other methods [46,47] need to be used. However, for any finite temperature, the long-time limit holds. For the considered limit $\omega_R > k_B T$, Eq. (59) stays the same and all diagrams decay in the same way. The convergence analysis gives in this case only one condition,

$$\frac{m\omega_R}{\epsilon_C k_B T} \ll 1. \quad (62)$$

We then obtain that even at very small temperatures, convergence can be achieved in the strong-coupling limit, $\epsilon_C \gg \omega_R$.

VI. CONCLUSIONS

We discussed a master-equation expansion where first the coupling to the bath is diagonalized explicitly and then expanded in the system operators dressed by the bath operators. The motivation here is to study expansion schemes that can be used in the case of strong coupling to the environment. We formally introduced contraction rules which allow for the division of all resulting terms in the expansion into two-time correlators of type $P(t_1, t_2)$ and four-time correlators, described by the connector $F(t_1, t_2, t_3, t_4)$. The introduced rules allowed for a consistent definition of the self-energy. We showed that

the contribution of the connector is important since it contains the effects of the slowly decaying correlations. We then derived explicit limits when the leading-order master-equation approach is valid, i.e., when the contribution from the two types of diagrams in higher orders stays small. The results clarify the limits of our previous works on lasing in systems under strong noise [19,20], incoherent Cooper-pair tunneling in Josephson-junction arrays [21], as well as inelastic Cooper-pair tunneling across voltage-biased Josephson junctions in the Coulomb blockade regime [22,23].

As we discussed in Sec. V A 1, the connection of the used noise spectral function to $1/f$ noise is interesting. Given a noise spectral function of Eq. (47), we can describe the high-frequency tail of $1/f$ noise,

$$S_{1/f, \text{high}} = \int_{\omega_{R, \text{min}}}^{\infty} d\omega_R \frac{1}{\omega_R} S(\omega) = \frac{2\epsilon_C k_B T [\pi - 2 \arctan(\omega_{R, \text{min}}/\omega)]}{\omega}, \quad (63)$$

where the low-frequency limit for the cutoff frequency ω_R is determined by the condition $m^2/\sqrt{\epsilon_C k_B T} \omega_{R, \text{min}} \ll 1$. Such connection can then be used to theoretically account for a large part of low-frequency noise, in limits where traditional direct system-bath coupling expansions do not work.

-
- [1] U. Weiss, *Quantum Dissipative Systems*, 3rd ed. (World Scientific, Singapore, 2008).
- [2] H. J. Carmichael, *Statistical Methods in Quantum Optics I*, 2nd ed. (Springer, New York, 2002).
- [3] Y. Makhlin, G. Schön and A. Shnirman, in *New Directions in Mesoscopic Physics (Towards Nanoscience)*, edited by R. Fazio, V. F. Gantmakher, and Y. Imry (Kluwer Dordrecht, The Netherlands, 2003), pp. 197–224.
- [4] G. Lindblad, *Commun. Math. Phys.* **48**, 119 (1976).
- [5] C. K. Lee, J. Moix, and J. Cao, *J. Chem. Phys.* **136**, 204120 (2012).
- [6] D. P. S. McCutcheon and A. Nazir, *New J. Phys.* **12**, 113042 (2010).
- [7] A. Chin and M. Turlakov, *Phys. Rev. B* **73**, 075311 (2006).
- [8] J. T. Devreese and A. S. Alexandrov, *Rep. Prog. Phys.* **72**, 066501 (2009).
- [9] H. Dekker, *Phys. Rev. A* **35**, 1436 (1987).
- [10] M. Thorwart, E. Paladino, and M. Grifoni, *Chem. Phys.* **296**, 333 (2004).
- [11] F. K. Wilhelm, S. Kleff, and J. von Delft, *Chem. Phys.* **296**, 345 (2004).
- [12] F. Nesi, E. Paladino, M. Thorwart, and M. Grifoni, *Phys. Rev. B* **76**, 155323 (2007).
- [13] F. Nesi, E. Paladino, M. Thorwart, and M. Grifoni, *Europhys. Lett.* **80**, 40005 (2007).
- [14] G.-L. Ingold and Yu. V. Nazarov, in *Single Charge Tunneling*, edited by H. Grabert and M. H. Devoret, NATO ASI Series B (Plenum, New York, 1992), Vol. 294, pp. 21–107.
- [15] A. Shnirman, G. Schön, I. Martin, and Y. Makhlin, *Phys. Rev. Lett.* **94**, 127002 (2005).
- [16] R. Harris, M. W. Johnson, S. Han, A. J. Berkley, J. Johansson, P. Bunyk, E. Ladizinsky, S. Govorkov, M. C. Thom, S. Uchaikin, B. Bumble, A. Fung, A. Kaul, A. Kleinsasser, M. H. S. Amin, and D. V. Averin, *Phys. Rev. Lett.* **101**, 117003 (2008).
- [17] T. Lanting, M. H. S. Amin, M. W. Johnson, F. Altomare, A. J. Berkley, S. Gildert, R. Harris, J. Johansson, P. Bunyk, E. Ladizinsky, E. Tolkacheva, and D. V. Averin, *Phys. Rev. B* **83**, 180502(R) (2011).
- [18] S. Boixo, V. N. Smelyanskiy, A. Shabani, S. V. Isakov, M. Dykman, V. S. Denchev, M. Amin, A. Smirnov, M. Mohseni, and H. Neven, *Nat. Commun.* **7**, 10327 (2016).
- [19] M. Marthaler, Y. Utsumi, D. S. Golubev, A. Shnirman, and G. Schön, *Phys. Rev. Lett.* **107**, 093901 (2011).
- [20] M. Marthaler, Y. Utsumi, and D. S. Golubev, *Phys. Rev. B* **91**, 184515 (2015).

- [21] J. H. Cole, J. Leppäkangas, and M. Marthaler, *New J. Phys.* **16**, 063019 (2014).
- [22] J. Leppäkangas, M. Fogelström, A. Grimm, M. Hofheinz, M. Marthaler, and G. Johansson, *Phys. Rev. Lett.* **115**, 027004 (2015).
- [23] J. Leppäkangas, M. Fogelström, M. Marthaler, and G. Johansson, *Phys. Rev. B* **93**, 014506 (2016).
- [24] P. P. Orth, A. Imambekov, and K. LeHur, *Phys. Rev. B* **87**, 014305 (2013).
- [25] O. Kashuba, D. M. Kennes, M. Pletyukhov, V. Meden, and H. Schoeller, *Phys. Rev. B* **88**, 165133 (2013).
- [26] M. Merkli, G. P. Berman, and R. Sayre, *J. Math. Chem.* **51**, 890 (2013).
- [27] A. Garg, J. N. Onuchic, and V. Ambegaokar, *J. Chem. Phys.* **83**, 4491 (1985).
- [28] I. Wilson-Rae and A. Imamoglu, *Phys. Rev. B* **65**, 235311 (2002).
- [29] M. Marthaler, J. Leppäkangas, and J. H. Cole, *Phys. Rev. B* **83**, 180505(R) (2011).
- [30] D. P. DiVincenzo and D. Loss, *Phys. Rev. B* **71**, 035318 (2005).
- [31] D. M. Kennes, O. Kashuba, and V. Meden, *Phys. Rev. B* **88**, 241110(R) (2013).
- [32] P.-Q. Jin, M. Marthaler, J. H. Cole, A. Shnirman, and G. Schön, *Phys. Rev. B* **84**, 035322 (2011).
- [33] H. Grabert, G.-L. Ingold, and B. Paul, *Europhys. Lett.* **44**, 360 (1998).
- [34] G.-L. Ingold and H. Grabert, *Phys. Rev. Lett.* **83**, 3721 (1999).
- [35] J. Leppäkangas, M. Marthaler, and G. Schön, *Phys. Rev. B* **84**, 060505(R) (2011).
- [36] A. Heimes, V. F. Maisi, D. S. Golubev, M. Marthaler, G. Schön, and J. P. Pekola, *Phys. Rev. B* **89**, 014508 (2014).
- [37] D. S. Golubev, M. Marthaler, Y. Utsumi, and G. Schön, *Phys. Rev. B* **81**, 184516 (2010).
- [38] J. Leppäkangas, G. Johansson, M. Marthaler, and M. Fogelström, *Phys. Rev. Lett.* **110**, 267004 (2013).
- [39] J. Zimmer, N. Vogt, A. Fiebig, S. V. Syzranov, A. Lukashenko, R. Schäfer, H. Rotzinger, A. Shnirman, M. Marthaler, and A. V. Ustinov, *Phys. Rev. B* **88**, 144506 (2013).
- [40] T. F. Ronnow, Z. Wang, J. Job, S. Boixo, S. V. Isakov, D. Wecker, J. M. Martinis, D. A. Lidar, and M. Troyer, *Science* **345**, 420 (2014).
- [41] P. Macha, G. Oelsner, J.-M. Reiner, M. Marthaler, S. Andre, G. Schön, U. Hübner, H.-G. Meyer, E. Ilichev, and A. V. Ustinov, *Nat. Commun.* **5**, 5146 (2014).
- [42] H. Schoeller and G. Schön, *Phys. Rev. B* **50**, 18436 (1994).
- [43] C. Karlewski and M. Marthaler, *Phys. Rev. B* **90**, 104302 (2014).
- [44] O.-P. Saira, M. Zgirski, K. L. Viisanen, D. S. Golubev, and J. P. Pekola, *Phys. Rev. Appl.* **6**, 024005 (2016).
- [45] G.-L. Ingold, H. Grabert, and U. Eberhardt, *Phys. Rev. B* **50**, 395 (1994).
- [46] O. Kashuba and H. Schoeller, *Phys. Rev. B* **87**, 201402(R) (2013).
- [47] R. B. Saptsov and M. R. Wegewijs, *Phys. Rev. B* **90**, 045407 (2014).